Recyclable Hydrogen Storage System Composed of Ammonia and Alkali Metal Hydride

Hikaru Yamamoto[1], Hiroki Miyaoka[2], Satoshi Hino[2], Haruyuki Nakanishi[3], Takayuki Ichikawa[1,2,]* and Yoshitsugu Kojima[1,2]

[1]*Department of Quantum Matter, AdSM, Hiroshima University, 1-3-1 Kagamiyama, Higashi-Hiroshima, Hiroshima, 739-8530, Japan*

[2]*Institute for Advanced Materials Research, Hiroshima University, 1-3-1 Kagamiyama, Higashi-Hiroshima, Hiroshima, 739-8530, Japan*

[3]*Higashi-Fuji Technical Center, Toyota Motor Corporation, 1200 Misyuku, Susono, Shizuoka, 410-1193, Japan*

Abstract (110/150)

Ammonia (NH_3) reacts with alkali metal hydrides *M*H (*M* = Li, Na, and K) in an exothermic reaction to release hydrogen (H_2) at room temperature, resulting that alkali metal amides (MNH_2) which are formed as by-products. In this work, hydrogen desorption properties of these systems and the condition for the recycle from MNH_2 back to *M*H were investigated systematically. For the hydrogen desorption reaction, the

reactivities of *M*H with NH_3 were better following the atomic number of *M* on the periodic table, Li < Na < K. It was confirmed that the hydrogen absorption reaction of all the systems proceeded under 0.5 MPa of H_2 flow condition below 300 °C.

Keywords: hydrogen storage systems, thermodynamic properties, ammonia, alkali metal hydrides, mechanical milling.

*Corresponding author. Tel. & Fax: +81-82-424-5744;

E-mail address: tichi@hiroshima-u.ac.jp. (T. Ichikawa)

Introduction

The development of the hydrogen storage and transportation technologies is a quite important issue to disperse a primary energy source. At present, compressed hydrogen gas, liquid hydrogen, and hydrogen storage materials are considered for the practical use [1]. Hydrogen storage materials can store the higher volumetric density of hydrogen compared to the gaseous and liquid hydrogen storage systems [2]. Therefore, the hydrogen storage materials are considered as a promising technology for not only on-board application but also for the stationary uses [1-5].

Sodium borohydride $NaBH_4$ is one of the attractive hydrogen storage materials because H_2 can be released with exothermic reaction by a hydrolysis reaction at room temperature as follows,

$$NaBH_4 + 2H_2O \rightarrow NaBO_2 + 4H_2 \quad (1).$$

Particularly, in the case of the $NaBH_4$ and H_2O system catalyzed by Pt-$LiCoO_2$, the hydrogen conversion of more than 90 % is obtained within 15 minutes as reported by Kojima *et al*. [6]. However, this system has a crucial problem with respect to a regeneration process of $NaBH_4$ and H_2O, namely, a high temperature over 1500 °C is required to recycle back to them from the by-product $NaBO_2$ [7].

Ammonia (NH_3) has a high hydrogen storage capacity of 17.8 mass% and it is easily

liquefied by compression at 1.0 MPa at room temperature. Therefore, NH_3 is thought to be one of the attractive hydrogen storage and transportation materials [8, 9]. However, a high temperature over 400 °C and a suitable catalyst are required to decompose NH_3 into hydrogen (H_2) and nitrogen (N_2) because NH_3 is kinetically stable material [10, 11], resulting that the practical application of NH_3 itself as a hydrogen storage material is limited. On the other hand, NH_3 is a polar molecule just like H_2O, thereby similar reaction to hydrolysis would be expected.

On the basis of the above background, a hydrogen storage system composed of NH_3 and lithium hydride (LiH) system have been designed as described by the following reaction,

$$LiH + NH_3 \leftrightarrow LiNH_2 + H_2 \quad (2).$$

The system has a high hydrogen capacity of 8.1 mass% and a suitable enthalpy change $|\Delta H| = 50 \pm 9$ kJ/mol H_2 for practical use [12, 13]. It is noticeable that the hydrogen desorption reaction can proceed even at room temperature due to hydrolysis-type exothermic reaction. For the recycle process of by-product $LiNH_2$ into LiH and NH_3, it is clarified that the reaction is occurred at 300 °C by removing NH_3 partial pressure under 0.5 MPa of H_2 flow [12]. Thus, the LiH-NH_3 system is recognized as a promising system with recyclable hydrogen storage system.

In this work, for the alkali metal hydrides *M*H (*M* = Li, Na, and K) and NH_3 systems, the hydrogen desorption properties at room temperature and the detailed condition for the recycle from *M*NH_2 back to *M*H are systematically investigated.

Experimental procedure

Lithium hydride (LiH) (99.4%, Alfa Aesar), Sodium hydride (NaH) (95%, Aldrich), Potassium hydride (KH) synthesized from Potassium (K) (99.95%, Aldrich) and H_2 (99.99999 %), Lithium amide ($LiNH_2$) (95%, Aldrich), Sodium amide ($NaNH_2$) (95%, Aldrich), and Potassium amide (KNH_2) synthesized form the KH and NH_3 (99.999 %) were used for the experiments in this work. The metal hydride *M*H (*M* = Li, Na, and K) samples were activated by milling for 10 hours under 1.0 MPa of H_2 pressure using a planetary ball mill apparatus (Fritsch, P7), where the activated *M*H samples are named as *M*H*. All the samples were handled in a glove box (Miwa MFG, MP-P60W) filled with a purified Ar (> 99.9999 %) to avoid an oxidation and hydration due to water.

The H_2 desorption properties of *M*H and NH_3 systems were investigated by the following process. A weighed amount of *M*H or *M*H* was packed into a closed pressure vessel in the glove box, then 0.5 MPa NH_3 with a molar ratio of NH_3/*M*H = 1 was introduced into the vessel. After that, the reaction of *M*H and NH_3 was proceeding at

room temperature for 10 minutes, 1, 12, and 24 hours under a static condition (closed system). In order to estimate the reaction yield during each reaction time, weight of the solid sample was measured before and after the reaction.

The H_2 absorption conditions of MNH$_2$ were examined as follows. Thermal analysis of MNH$_2$ by using differential scanning calorimetry (DSC) (TA Instruments, Q10 PDSC) installed in a glove box (Miwa MFG, DBO-1.5KP) were carried out under 0.5 MPa of H_2 or Ar flow condition with a heating rate of 5 °C/minute to search the reaction temperature between MNH$_2$ and H_2. From the DSC profile under H_2 and Ar flow, the hydrogenation temperature was determined. After that, a weighed MNH$_2$ was treated at the designated temperature based on the above thermal analyses for 4 hours under H_2 flow condition (open system) to examine the reactivities. The sample masses before and after the experiments were measured to calculate the reaction yield.

The products after the H_2 desorption and absorption reaction were identified by X-ray diffraction (XRD) measurement (Rigaku, RINT-2100, CuKα radiation), where the samples were covered by a polyimide sheet (Du Pont-Toray Co., LTD., Kapton®) to protect the samples from an oxidation during XRD measurements.

Results and discussion

Hydrogen desorption properties

Figure 1 shows XRD patterns of (a) LiH/LiH*, (b) NaH/NaH*, and (c) KH/KH* before and after reaction with NH_3 (0.5 MPa) at room temperature, where *M*H* denotes the milled metal hydrides. XRD patterns of possible hydride, amide, oxide, and hydroxide available in the database are shown as references. After the reaction of each hydride with NH_3, the diffraction peaks corresponding to each amide phase were observed as shown in Fig. 1 (a), (b), and (c), indicating that the hydrogen desorption reaction proceeded even at room temperature for all the systems. From the XRD patterns of LiH* and NaH*, it is noticed that the diffraction peaks of hydrides are weakened and broadened by ball milling for 10 hours. The XRD results indicate that the mean grain size (crystallite size) is reduced and the distortion for the crystal structure is introduced by the mechanical energy. As shown in the XRD patterns of LiH* and NaH* after the reaction with NH_3, the diffraction peaks assigned to $LiNH_2$ and $NaNH_2$ were distinct. In the case of KH*, the XRD pattern before/after the reaction was almost the same as that of KH without the milling. However, the diffraction peaks of hydride completely disappeared for KH* after the reaction with NH_3, in which the peak around 31 ° was especially characteristic. Therefore, it is expected that the reaction kinetics for

the hydrogen desorption reaction are improved by the ball milling.

In Figure 2, hydrogen generation yields by the reaction between *M*H/*M*H* and NH_3 are shown as a function of the reaction time. The reaction yield for 24 hours of the un-milled LiH and NaH were about 12 and 23 %, respectively. After ball-milling, the initial reactivity of them were significantly enhanced, then the respective reaction yield of LiH* and NaH* reached up to 53 and 60 % in 24 hours. In the case of KH, the fastest reaction was revealed among *M*H as shown in Fig. 2. Only 1 hour was enough to reach more than 80 % of reaction yield even before ball-milling. Furthermore, it is noted that the reaction yield of KH* is almost 100 % after 12 hours reaction.

From the above experimental facts, it is confirmed that the reaction yield of the hydrogen desorption reactions between *M*H and NH_3 is better in the order of Li < Na < K. In addition, the ball-milling as a pre-treatment enhances the reaction yield. The ball-milling in general introduces a reduction of crystal grain size, an increase in surface area, an induction of defects and distortion, an exfoliation of oxide and/or hydroxide layer on the surface of *M*H [12]. Thus, it is expected that the above effects would lead the activation of the *M*H for the reaction with NH_3.

Hydrogen absorption properties

In order to investigate the hydrogen absorption properties of metal amides MNH_2, the thermal analysis by DSC under 0.5 MPa of H_2 flow were performed. In addition to the above measurements, the thermal analysis of each amide under Ar flow condition was performed for comparison. Here, Gibbs free energy ΔG on the reactions $MNH_2 + H_2 \rightarrow MH + NH_3$ is expressed as follows,

$$\Delta G = \Delta H - T\Delta S^0 - TR\ln\left(\frac{p_{H_2}}{p_{NH_3}}\right), \tag{3}$$

where ΔH is the enthalpy change, ΔS^0 is the standard entropy change, R is the gas constant, p_{H2} is partial pressure of H_2, and p_{NH3} is partial pressure of NH_3. Under the H_2 flow condition in an open system, absolute value of the last entropy term in equation (3) is increased by reducing partial pressure p_{NH3}, indicating that the equilibrium condition of the reaction is changed. As a result, it is expected that the reaction proceeds at lower temperature compared with that in a closed system. The results of DSC measurements for $LiNH_2$, $NaNH_2$, and KNH_2 are shown in Figure 3. This apparatus has no cooling system, leading to a gradual change of the background on the cooling process from about 100 and 150 °C under H_2 and Ar flow, respectively. For $LiNH_2$, the DSC profile under H_2 flow was almost the same as that under Ar flow as shown in Fig. 3 (a). Thus, it was difficult to determine the reaction temperature with H_2. However, it was confirmed by XRD measurement that LiH phase was formed by the reaction after the measurement

under H_2 flow, indicating that $LiNH_2$ can react with H_2 to form LiH and NH_3 by the heating up to 300 °C. In the DSC profile of $NaNH_2$ obtained under Ar flow, two endothermic peaks and two corresponding exothermic peaks were observed in the heating and cooling process, respectively. This result indicates that two phase transitions were occurred around 150 and 200 °C, where the phase transition around 200 °C should be a melting [14]. Under H_2 flow, it is noticed that a gradual endothermic reaction starts around 100 °C as shown in the upper part of Fig. 3 (b). In the cooling process, the peaks due to the phase transitions completely disappeared, suggesting that $NaNH_2$ reacted with H_2 and changed into NaH during the heating up to 200 °C. In the case of KNH_2, the endo/exothermic peaks corresponding to a phase transition were clearly observed around 60 and 80 °C under Ar flow in the heating and cooling processes. In the case of H_2 flow, a broad endothermic peak appeared in the temperature range from 50 to 250 °C in the heating process as shown in the upper part of Fig. 3 (c), where the sharp endothermic peak around 60 °C overlapped with the broad peak may be caused by the phase transition of the remaining KNH_2. Moreover, no peaks appear in this case in contrast to the DSC under Ar in the cooling process, suggesting that the gradual endothermic peak would be originated in the hydrogenation of KNH_2.

On the basis of the above thermal analyses, all the MNH$_2$ samples were treated at the

designated temperature for 4 hours under H_2 flow condition by using DSC apparatus. Figure 4 shows XRD patterns of (a) $LiNH_2$, (b) $NaNH_2$, and (c) KNH_2 before and after the hydrogenation treatments. From the results, it was clear that the diffraction peaks corresponding to each amide observed before the reaction were changed to the peaks of each hydride after the reaction. The results indicate that all the amides can be recycled back into the hydrides by the reaction with 0.5 MPa H_2 under flow condition below 300 °C.

The reaction yield on the hydrogen absorption reaction of MNH_2 for 4 hours at 50, 100, 200, and 300 °C are shown in Table 1. For $LiNH_2$, 300 °C was required to obtain more than 70 % of the reaction yield. On the other hand, the reaction yield of $NaNH_2$ and KNH_2 was more than 90 % even at 200 °C. Noticeably, it was confirmed that the reaction of KNH_2 and H_2 started from 50 °C, and then the reaction yield was estimated to be about 20 %. It can be suggested that the above results correspond with the hydrogen absorption properties of MNH_2 analyzed by DSC.

Conclusions

In this work, the hydrogen desorption at room temperature under the static condition and the hydrogen absorption in the temperature range from 50 to 300 °C under H_2 flow

condition on *M*H and NH_3 systems ($MH + NH_3 \leftrightarrow MNH_2 + H_2$) were demonstrated. For the hydrogen desorption in the closed system, all the hydrides react with NH_3 and form the corresponding amides and H_2 even at room temperature. The reaction kinetics is better in order of atomic number of alkali metal element of the periodic table, Li < Na < K. In addition, the mechanical milling enhances the reactivity of *M*H with NH_3. For the hydrogen absorption in the opened system, it is confirmed by the XRD measurements that "*all*" the amide phases can be recycled back to the corresponding hydride phases. In order to obtain more than 70 % of reaction yield, $LiNH_2$, $NaNH_2$, and KNH_2 require 300, 200, and 100 °C, respectively. From the above results, the KH-NH_3 system exhibits the best reactivity for both of the hydrogen desorption and absorption reactions among the systems. However the hydrogen capacity in KH-NH_3 system is less than the other systems. Therefore, an improvement of the kinetics for LiH-NH_3 system containing higher amount of hydrogen would be a future prospect.

From the experimental facts in this work, it is shown that the *M*H-NH_3 systems are very promising cyclic-hydrogen ab/desorption system working at relatively low temperature for practical application.

Acknowledgement

The authors gratefully acknowledge Dr. Hironobu Fujii, Dr. Biswajit Paik, and Mr. Kyoichi Tange for the good discussion and valuable help in this work.

References

[1] Züttel A. Hydrogen storage and distribution systems, Mitig. Adapt. Strat. Glob. Change 2007; 12: 343-365.

[2] Schlapbach L and Züttel A. Hydrogen-storage materials for mobile applications, Nature 2001; 414: 353-358.

[3] Akiba E. Hydrogen-absorbing alloys, Current Opinion in Solid State & Materials Science 1999; 4: 267-272.

[4] Sandrock G. A panoramic overview of hydrogen storage alloys from a gas reaction point of view, J Alloys Compd 1999; 295: 877-888.

[5] Grochala W and Edwards PP. Thermal decomposition of the non-interstitial hydrides for the storage and production of hydrogen, Chemical Reviews 2004; 104: 1283-1315.

[6] Kojima Y, Suzuki K, Fukumoto K, Sasaki M, Yamamoto T, Kawai Y and Hayashi H. Hydrogen generation using sodium borohydride solution and metal catalyst coated on metal oxide, Int J Hydrogen Energy 2002; 27: 1029-1034.

[7] Kojima Y and Haga T. Recycling process of sodium metaborate to sodium borohydride, Int J Hydrogen Energy 2003; 28: 989-993.

[8] Strickland G. Hydrogen derived from ammonia: Small-scale costs, Int J Hydrogen Energy 1984; 9: 759-766.

[9] Avery WH. A role for ammonia in the hydrogen economy, Int J Hydrogen Energy 1988; 13: 761-773.

[10] Choudhary TV, Sivadinarayana C and Goodman DW. Catalytic ammonia decomposition: COx-free hydrogen production for fuel cell applications, Catal Lett 2001; 72: 197-201.

[11] Yin SF, Xu BQ, Zhou XP and Au CT. A mini-review on ammonia decomposition catalysts for on-site generation of hydrogen for fuel cell applications, Applied Catalysis A: General 2004; 277: 1-9.

[12] Kojima Y, Tange K, Hino S, Isobe S, Tsubota M, Nakamura K, Nakatake M, Miyaoka H, Yamamoto H and Ichikawa T. Molecular hydrogen carrier with activated nanohydride and ammonia, J Mater Res 2009; 24: 2185-2190.

[13] Hino S, Ogita N, Udagawa M, Ichikawa T and Kojima Y. Thermodynamic properties of lithium amide under hydrogen pressure determined by Raman spectroscopy, J Appl Phys 2009; 105: 023527.

[14] Lide RD, *CRC Handbook of Chemistry and Physics*. 89th ed. 2008, New York.

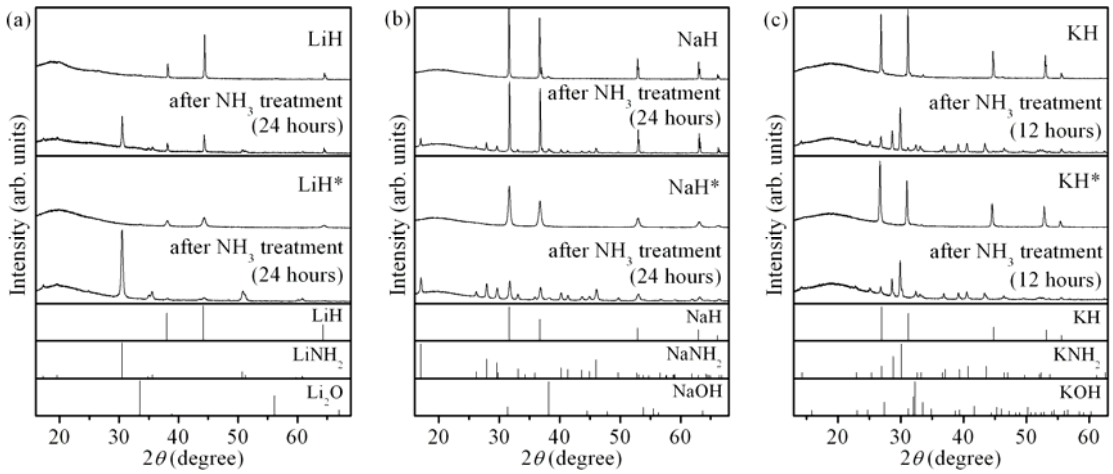

Figure 1 XRD patterns of (a) LiH/LiH*, (b) NaH/NaH*, and (c) KH/KH* before and after reaction with NH_3 (0.5 MPa) at room temperature. As reference, XRD patterns of LiH (PDF #65-2987), $LiNH_2$ (PDF #71-1616), Li_2O (PDF #65-2972), NaH (PDF #76-0171), $NaNH_2$ (PDF #85-0401), NaOH (PDF #35-1009), KH (PDF #54-0410), KNH_2 (PDF #19-0934), and KOH (PDF #78-0190) in the database are shown.

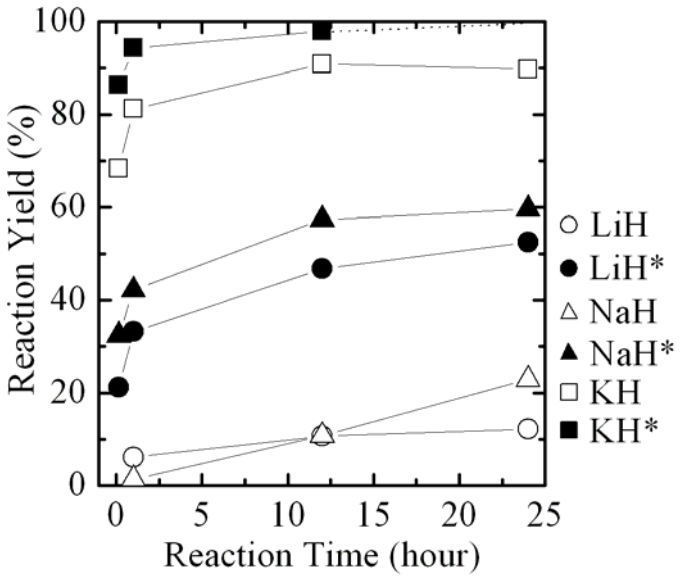

Figure 2 Hydrogen generation profiles for the reactions of *M*H/*M*H* with NH_3.

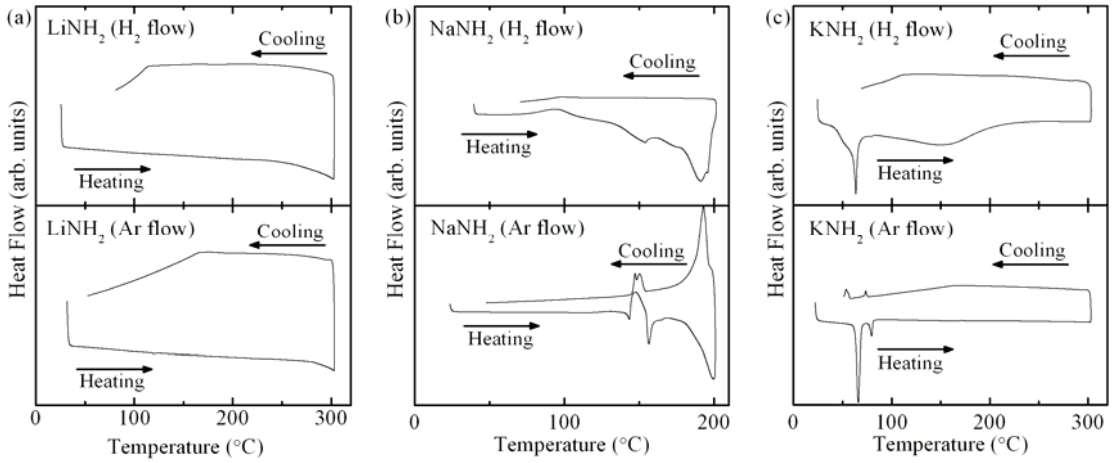

Figure 3 DSC profiles of (a) $LiNH_2$, (b) $NaNH_2$, and (c) KNH_2 under 0.5 MPa of (upper) H_2 flow and (lower) Ar flow condition.

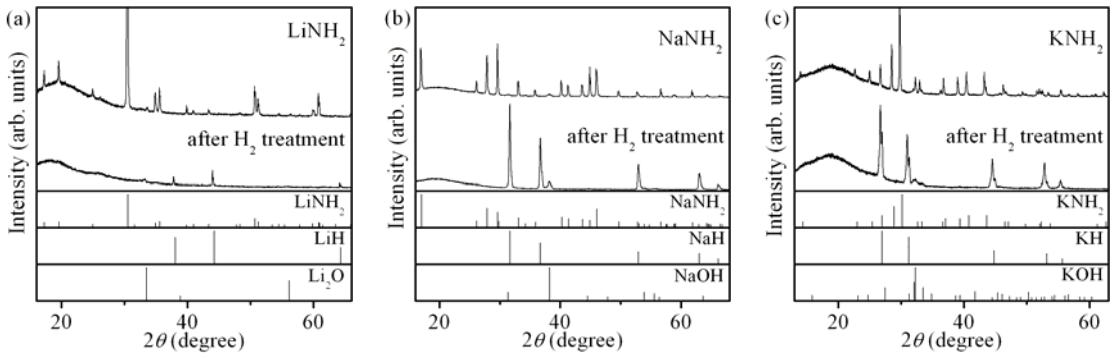

Figure 4 XRD patterns of MNH_2 before and after the treatment under H_2 flow condition for 4 hours: (a) $LiNH_2$ at 300 °C, (b) $NaNH_2$ at 200 °C and (c) KNH_2 at 200 °C. As reference, XRD patterns of $LiNH_2$ (PDF #71-1616), LiH (PDF #65-2987), Li_2O (PDF #65-2972), $NaNH_2$ (PDF #85-0401), NaH (PDF #76-0171), NaOH (PDF #35-1009), KNH_2 (PDF #19-0934), KH (PDF #54-0410), and KOH (PDF #78-0190) in the database are shown.

Table 1 Reaction yield of the reaction between MNH_2 (M = Li, Na, and K) and H_2 at different temperature for 4 hours.

Temperature	$LiNH_2$	$NaNH_2$	KNH_2
50 °C	0 %	3.6 %	19.2 %
100 °C	0 %	13.8 %	78.8 %
200 °C	4.2 %	94.1 %	91.2 %
300 °C	71.0 %	-*	100 %

*$NaNH_2$ can not be treated at 300 °C because its melting point is around 200 °C